

## Research report

Automated voxel- and region-based analysis of gray matter and cerebrospinal fluid space in primary dementia disorders<sup>☆</sup>

Karl Egger<sup>a,\*</sup>, Alexander Rau<sup>a</sup>, Shan Yang<sup>a</sup>, Stefan Klöppel<sup>b</sup>, Ahmed Abdulkadir<sup>b</sup>, Elias Kellner<sup>c</sup>, Lars Frings<sup>d</sup>, Sabine Hellwig<sup>d,e</sup>, Horst Urbach<sup>a</sup>, for the Alzheimer's Disease Neuroimaging Initiative

<sup>a</sup> Department of Neuroradiology, Medical Center – University of Freiburg, Faculty of Medicine, University of Freiburg, Breisacher Straße 64, 79106 Freiburg, Germany

<sup>b</sup> University Hospital of Old Age Psychiatry and Psychotherapy, University of Bern, Hochschulstrasse 6, 3012 Bern, Switzerland

<sup>c</sup> Department of Radiology, Medical Center – University of Freiburg, Faculty of Medicine, University of Freiburg, Breisacher Straße 64, 79106 Freiburg, Germany

<sup>d</sup> Department of Nuclear Medicine, Medical Center – University of Freiburg, Faculty of Medicine, University of Freiburg, Breisacher Straße 64, 79106 Freiburg, Germany

<sup>e</sup> Department of Psychiatry and Psychotherapy, Medical Center – University of Freiburg, Faculty of Medicine, University of Freiburg, Hauptstraße 5, 79104 Freiburg, Germany

## HIGHLIGHTS

- Neurodegenerative diseases show different atrophy patterns on MRI.
- Voxel-based volumetry of 360 healthy controls and 120 patients with different dementia was performed.
- Dementia could be differentiated from normal ageing with high accuracy.
- Diagnostic accuracy is raised by investigating both grey matter and cerebrospinal fluid rather than grey matter only.

## ARTICLE INFO

## Keywords:

Dementia  
Alzheimer's disease  
Frontotemporal dementia  
Lewy body dementia  
Machine learning  
Volumetry

## ABSTRACT

**Purpose:** Previous studies showed voxel-based volumetry as a helpful tool in detecting pathologic brain atrophy. Aim of this study was to investigate whether the inclusion of CSF volume improves the imaging based diagnostic accuracy using combined automated voxel- and region-based volumetry.

**Methods:** In total, 120 individuals (30 healthy elderly, 30 frontotemporal dementia (FTD), 30 Alzheimer's dementia (AD) and 30 Lewy body dementia (LBD) patients) were analyzed with voxel-based morphometry and compared to a reference group of 360 healthy elderly controls. Abnormal GM and CSF volumes were visualized via z-scores. Volumetric results were finally evaluated by ROC analyses.

**Results:** Based on the volume of abnormal GM and CSF voxels high accuracy was shown in separating dementia from normal ageing (AUC 0.93 and 0.91, respectively) within 5 different brain regions per hemisphere (frontal, medial temporal, temporal, parietal, occipital). Accuracy for separating FTD and AD was higher based on CSF volume (FTD: AUC 0.80 vs. 0.75 in frontal regions; AD: AUC 0.78 vs. 0.68 in parietal regions based on CSF and GM respectively).

**Conclusions:** Differentiation of dementia patients from normal ageing persons shows high accuracy when based on automatic volumetry alone. Evaluating volumes of abnormal CSF performed better than volumes of abnormal GM, especially in AD and FTD patients.

**Abbreviations:** AD, Alzheimer's disease; FTD, frontotemporal dementia; LBD, Lewy body dementia; VBM, voxel based morphometry; SPM, statistical parametric mapping; CVR, combined voxel- and region-based; ROC, receiver operating characteristic; AUC, area under curve; PA, posterior atrophy; MTA, medial temporal atrophy; HC, healthy controls; MoCA, Montreal Cognitive Assessment; MPAGE, magnetization prepared rapid gradient echo; ROI, region of interest

\* A part of the data used in preparation of this article were obtained from the Alzheimer's Disease Neuroimaging Initiative (ADNI) database ([adni.loni.usc.edu](http://adni.loni.usc.edu)). As such, the investigators within the ADNI contributed to the design and implementation of ADNI and/or provided data but did not participate in analysis or writing of this report. A complete listing of ADNI investigators can be found at: [http://adni.loni.usc.edu/wp-content/uploads/how\\_to\\_apply/ADNI\\_Acknowledgement\\_List.pdf](http://adni.loni.usc.edu/wp-content/uploads/how_to_apply/ADNI_Acknowledgement_List.pdf).

\* Corresponding author at: Department for Neuroradiology, Medical Center – University of Freiburg, Breisacher Str. 64, 79106 Freiburg i. Breisgau, Germany.

E-mail address: [karl.egger@uniklinik-freiburg.de](mailto:karl.egger@uniklinik-freiburg.de) (K. Egger).

<https://doi.org/10.1016/j.brainres.2020.146800>

Received 21 October 2019; Received in revised form 26 February 2020; Accepted 20 March 2020

Available online 22 March 2020

0006-8993/© 2020 The Authors. Published by Elsevier B.V. This is an open access article under the CC BY license (<http://creativecommons.org/licenses/by/4.0/>).

## 1. Introduction

According to the German S3-Guideline Dementia (AWMF-Register-Number: 038-013) a cranial CT or MRI should be performed to exclude secondary causes such as tumor, subdural hemorrhage or hydrocephalus, and to contribute in differentiation of neurodegenerative disorders. For completing the first task, a CT is considered as sufficient. For the differentiation of neurodegenerative diseases, especially in

clinically unclear cases and younger patients, MRI is more favorable, since different pathologies such as Alzheimer's dementia (AD), frontotemporal dementia (FTD) and Lewy body dementia (LBD) show different atrophy pattern (Wippold et al., 2015).

When including depressive pseudodementia, treatable causes are found in up to 30% of patients (Djukic et al., 2015; Muangpaisan et al., 2012). Especially in these cases MRI might be a helpful tool to prove or exclude brain atrophy. Although published results show that visual

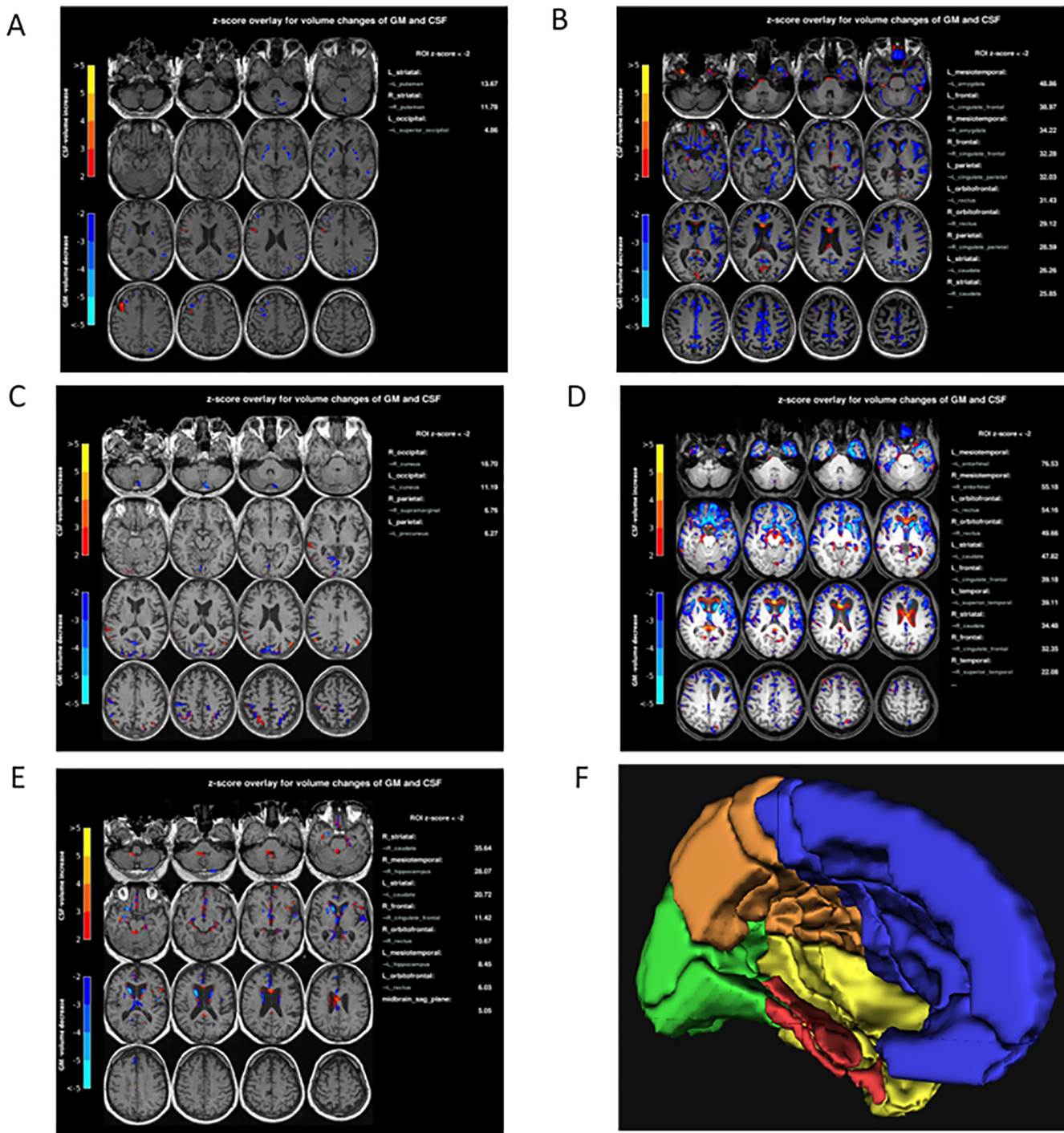


**Fig. 1.** Voxels with abnormal z-scores superimposed in dark to light blue (=GM-volume loss) and red to yellow (=CSF-volume increase) onto the individual 3D-T1w MRI. (A) HC (65F) without relevant cortical atrophy. (B) AD patient (71F) with typical medial temporal and parietal volume changes. (C) AD patient (72 M) with no atrophy within the medial temporal structures but significant CSF-volume increase within the parietal region. (D) FTD patient (52 M) with left temporopolar dominant atrophy. (E) DLB patient (74 M) with no pathognomonic atrophy pattern. (F) Template of one hemisphere depicted from a medial projection. Overview of the analyzed regions summarized using the LPBA 40 atlas to be comparable with the visual rating scales: frontal in blue, medial temporal in red, temporal in yellow, parietal in orange and occipital in green. CVR, combined voxel and region based; AD, Alzheimer's disease; GM, gray matter, CSF, cerebro spinal fluid.

rating as well as automated voxel-wise volumetric approaches hold diagnostic potential (Möller et al., 2014; Klöppel et al., 2015; Huppertz et al., 2016), diagnostic accuracy of MRI is rather low in daily clinical practice. One primary reason might be the lack of sensitivity and specificity of visual atrophy rating, even when established visual rating scales are applied (Davies et al., 2006; Scheltens et al., 1992; Koedam et al., 2011). Other reasons are a long post-processing time and a not standardized presentation of automated volumetric results (Frisoni et al., 2017). One of the most common used automated MRI post-processing approaches is Voxel-Based Morphometry (VBM) using Statistical Parametric Mapping (SPM) software (Ashburner, 2012). VBM is a method in which usually 3D T1-weighted MR images are transformed into a common space to get rid of the variability in brain anatomy among individuals. Before comparing brain volumes, data must be corrected for physiological differences such as head size, gender and age. Based on this principle, VBM has become a promising and well established biomarker in the differentiation of neurodegenerative diseases with respect to gray matter volume loss (Frisoni et al., 2017; Meeter et al., 2017; Saeed et al., 2017). VBM is methodologically sufficient for the classification of GM and WM as well as for clinical use. The evaluation was carried out several times with the result that the VBM is reproducible and stable and thus established as a standard method (Huppertz et al., 2010; Kazemi and Noorizadeh, 2014; Fellhauer et al., 2015).

Although visual rating scales are considered to evaluate gray matter volume loss, they are more or less based on the evaluation of widening of the corresponding brain sulci (Harper et al., 2016). We therefore hypothesized that the diagnostic accuracy in detecting region-specific pathologic brain atrophy can be improved by including voxel-wise evaluation of CSF volume into a volumetric MRI post-processing approach.

Therefore, aim of this study was to investigate the diagnostic accuracy in differentiating between dementia patients and healthy controls, as well as to differentiate between common primary dementia disorders by using combined voxel- and region-based (CVR) analyses of GM volume decrease and CSF volume increase.

## 2. Results

Human rating did only reach moderate accuracy in differentiating dementia patients from healthy controls with respect to medial temporal and parietal regions (AUC 0.79 and 0.71).

In differentiating the entities from each other, there was only moderate accuracy, too.

Low visual rating scores in the frontal (AUC 0.75) and temporal (AUC 0.73) regions were pathognomonic for FTD, while AD was delimited through medial temporal (AUC 0.76) and parietal (AUC 0.73) atrophy (Fig. 4).

### 2.1. Dementia versus normal aging

Receiver operating characteristic (ROC) analyses showed a high diagnostic accuracy when decreased GM volumes (z-score < -2) of the medial temporal lobes (area under the curve (AUC) 0.93) and of the temporal lobes (AUC 0.91) were considered. Diagnostic accuracy was lower, when the parietal (AUC 0.86), frontal (AUC 0.84) and occipital lobes (AUC 0.83) were considered, respectively (Fig. 2).

With respect to the CSF volume increase (z-score > 2) diagnostic accuracy was high for medial temporal regions (AUC 0.91) and moderate for temporal (AUC 0.84), parietal (AUC 0.84), frontal (AUC 0.73) and occipital regions (AUC 0.73) (Fig. 3). Based on these ROC curves, a sensitivity of 0.81 and specificity of 0.97 with respect to the GM volume, and a sensitivity of 0.83 and specificity of 0.9 with respect to the CSF volume within the medial temporal region was calculated.

Given the phenotypical variability of AD patients, atypical cases such as posterior atrophy (PA) were identified via a CSF volume

increase in the parietal lobes while medial temporal regions showed normal GM and CSF volumes.

### 2.2. FTD versus rest

ROC analyses revealed a moderate diagnostic accuracy with respect to the GM volume in temporal (AUC 0.78) and frontal regions (AUC 0.75). Corresponding values for the CSF volume were 0.81 and 0.8, respectively. Sensitivity and specificity for the temporal regions were 0.77 and 0.73 (GM volume) and 0.8 and 0.74 (CSF volume), respectively (Figs. 2 and 3).

### 2.3. AD versus rest

ROC analyses revealed a low accuracy when the GM volumes of the parietal lobes (AUC 0.67) and a moderate accuracy (AUC 0.78) when the CSF volumes were considered. This resulted in a sensitivity and specificity of 0.93 and 0.48 based on the GM volume and 0.73 and 0.76 for the CSF volume in parietal regions, respectively. Frontal and temporal regions showed low accuracy considering GM (AUC 0.67 and 0.65) with moderate accuracy using CSF (AUC 0.75 and 0.71) (Figs. 2 and 3).

### 2.4. LBD versus rest

ROC analyses of GM and CSF z-score-volumes showed a low accuracy with a maximum AUC of 0.58 and 0.55 in medialtemporal regions, quite close to chance level. The other regions have an even lower AUC (Figs. 2 and 3).

## 3. Discussion

Most previous VBM studies primarily assessed regional GM volume loss. In contrast, visual rating is typically based on defining abnormal regional widening of cortical sulci (Davies et al., 2006; Scheltens et al., 1992; Koedam et al., 2011). Here, we included information about the intracranial CSF volume into a VBM analysis in order to improve the diagnostic accuracy, especially to identify AD and FTD patients (Fig. 1).

After optimizing the threshold settings as visualized in the ROC curve (Figs. 2 and 3) the high true positive (TPR = sensitivity) and low false positive rates (FPR = 1-specificity) prove this analysis suited to detect and exclude abnormal brain volume conditions just by using the z-score-analysis output. Especially when separating AD and FTD patients from the remaining cohort, the additional CSF volume analysis of the parietal region in AD and frontal and temporal regions in FTD increased the diagnostic accuracy (Figs. 1 and 3). This approach surpasses human performance based on established visual rating scales.

Parietal atrophy is common in AD: In a former study, 28% of AD patients had prominent parietal atrophy without evident medial temporal lobe atrophy (MTA). Combining visual rating scales for MTA and posterior cortical atrophy increased the sensitivity to identify AD patients from around 50% to 73% (Koedam et al., 2011).

Rating of MTA and PA is mainly based on an increase of the CSF compartment. In the MTA score, first signs for atrophy of medial temporal structures are widening of the choroidal fissure and the temporal horn (Scheltens et al., 1992). The PA score is based on widening of the parietal sulci including the posterior cingulate and the parieto-occipital sulci evaluated in three different planes (Koedam et al., 2011). Current studies describe atrophies in both regions as pathognomonic for AD diagnosis (Frenzel et al., 2020; Cajanus et al., 2018; Hedderich et al., 2020; Cavedo et al., 2017; Persson et al., 2017).

Regarding FTD different quantification methods including VBM and region-based GM volumetry are established. A decision support tool named Disease State Index was used as statistical classifier. By using GM volumes of various brain areas and VBM, a classification sensitivity of up to 60% for the whole FTD cohort was achieved (Cajanus et al.,

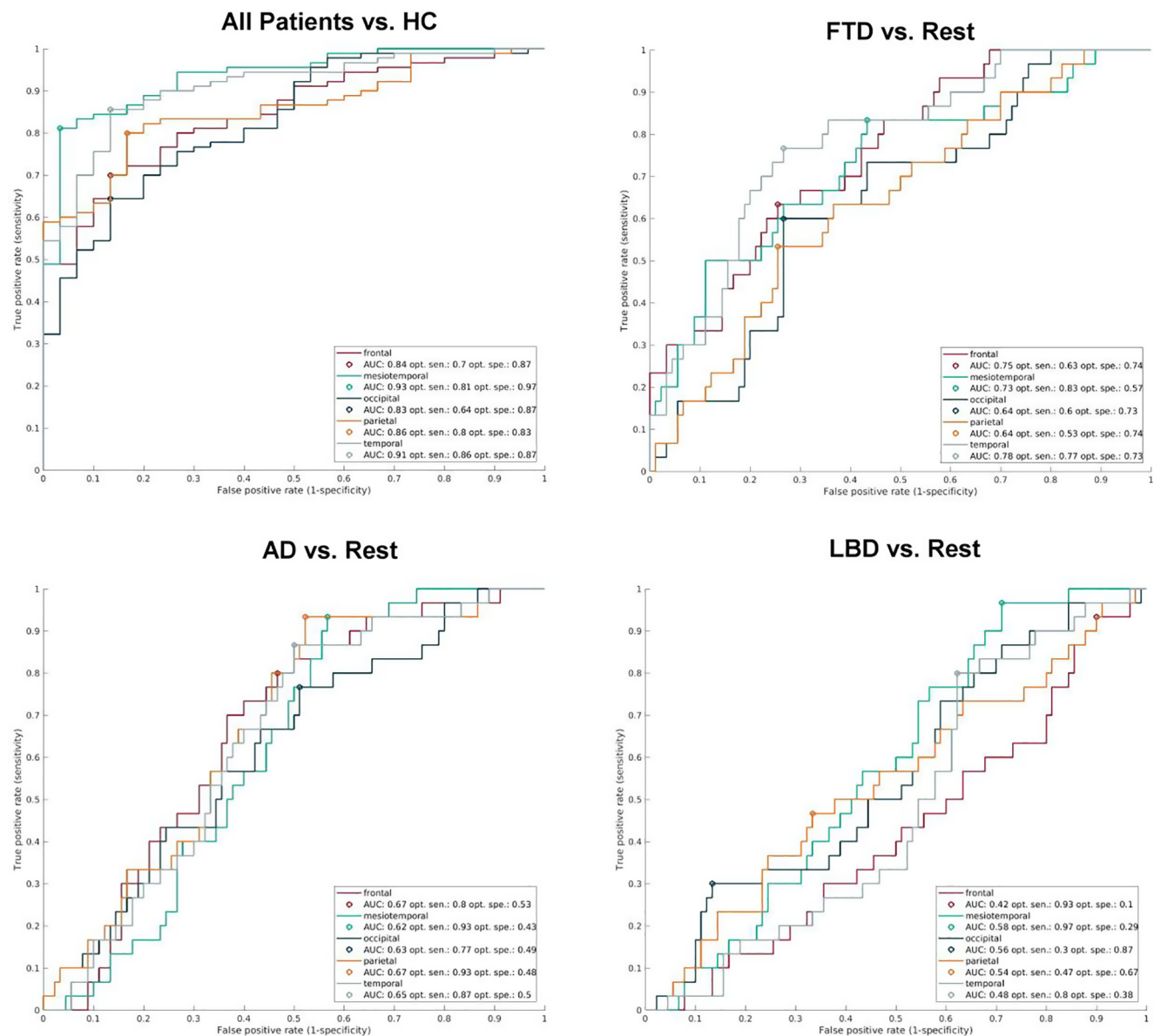


**Fig. 2.** ROC analyses based on GM CVR volumetry. ROC analyses based on the volume of voxels with z-score < -2 within the GM of frontal regions (red), medial (mesio) temporal regions (green), occipital regions (black), parietal regions (orange), temporal regions (gray). Maximum sensitivity (opt. sen.) and maximum specificity (opt. spe.) is shown as small circle on the corresponding curve representing the intercept with a 45 degree line closest to the error-free point (0.1). ROC, receiver operating characteristic; CVR, combined voxel and region based; GM, gray matter; HC, healthy control; FTD, frontotemporal dementia; AD, Alzheimer's disease; LBD, Lewy body dementia; AUC, area under the curve; opt. sen., optimized sensitivity; opt. spe., optimized specificity.

2018). This result is in accordance with our study regarding FTD classification when restricted to GM volume. However, with additional CSF volume analysis the sensitivity increased up to 93% (Fig. 3).

LBD patients were poorly identified with automated volumetry, regardless if CSF volume analysis was included or not. This is consistent with the existing literature and primarily due to the fact, that LBD is associated with only minimal volume changes on structural MRI as shown in autopsy confirmed cases (Nedelska et al., 2015).

Inter-scanner variability is considered a limitation for automated structural MRI based diagnostic decision support tools. However, this is mainly a problem in monitoring subtle longitudinal intra-individual volume changes (Huppertz et al., 2010). Since it is quite impossible to collect enough scans for preparing hard- and software-specific reference groups, we decided to include images from different scanners with different magnetic field strengths as well as to include images from the Alzheimer's Disease Neuroimaging Initiative cohort. However, the availability of fast and reliable automated volumetric results as well as

the additional effort for supporting the IT-infrastructure might be limiting factors for the region wide implementation into diagnostic routine. Therefore, institutional networking might help. As in our specific CVR volumetric algorithm, the total analysis time is about 10 min per case and via already existing secured internet connections images and volumetric results can be shared in a standardized way with relatively low effort.

#### 4. Conclusion

The focus of most volumetric studies is primarily on GM volume loss. In contrast, visual rating is typically based on defining abnormal widening of specific cortical sulci. Therefore, we added information on global intracranial CSF volume into the automated CVR-volumetric analyses and could therefore improve the diagnostic accuracy especially in AD as well as FTD patients.

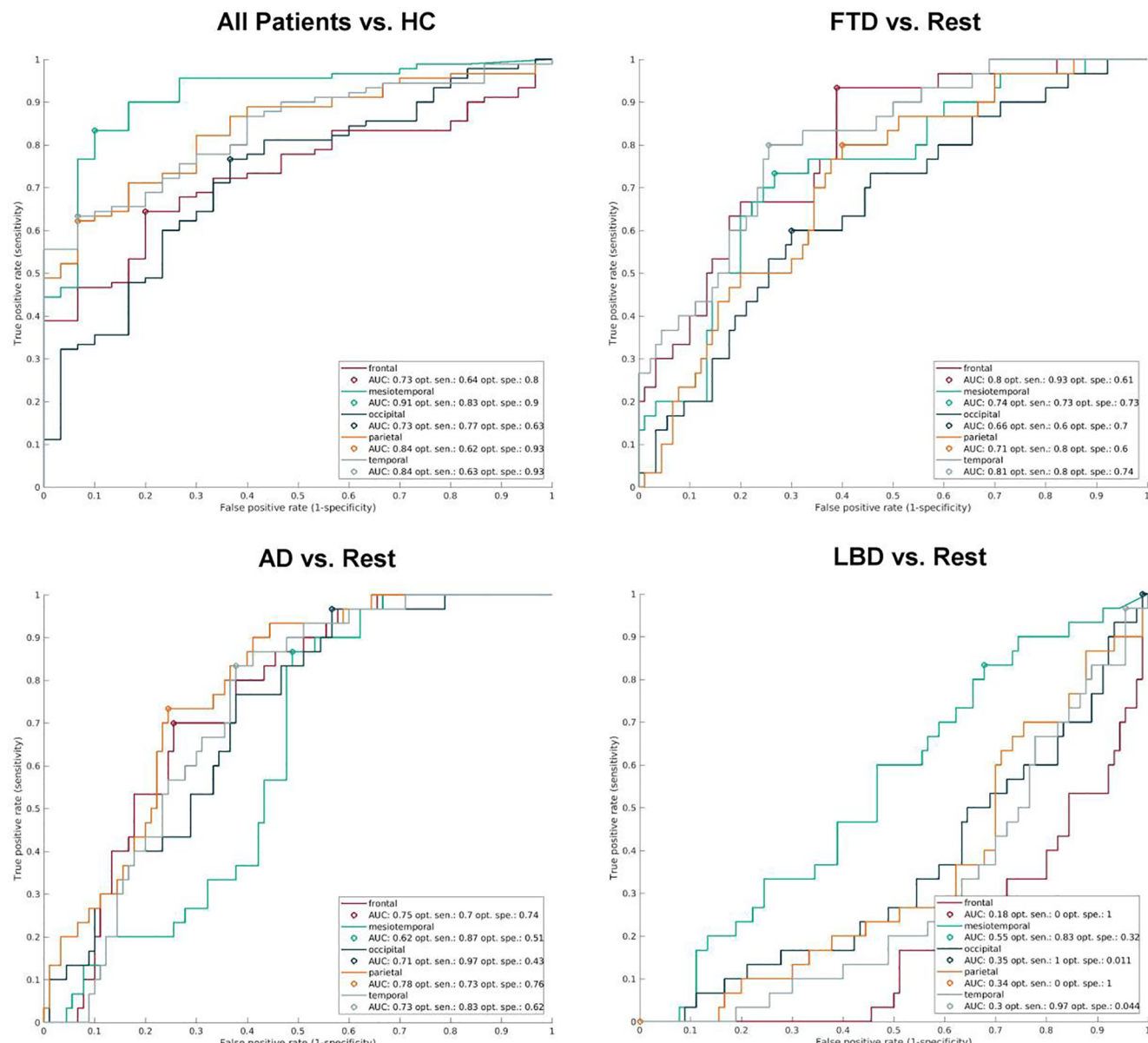


**Fig. 3.** ROC-analyses based on CSF CVR volumetry. ROC analyses based on the volume of voxels with z-score > 2 within the CSF space next to frontal regions (red), medial (mesio) temporal regions (green), occipital regions (black), parietal regions (orange), temporal regions (gray). Maximum sensitivity (opt. sen.) and maximum specificity (opt. spe.) is shown as small circle on the corresponding curve representing the intercept with a 45 degree line closest to the error-free point (0.1). ROC, receiver operating characteristic; CVR, combined voxel and region based; CSF, cerebro spinal fluid; HC, healthy control; FTD, frontotemporal dementia; AD, Alzheimer's disease; LBD, Lewy body dementia; AUC, area under the curve; opt. sen., optimized sensitivity; opt. spe., optimized specificity.

## 5. Methods

### 5.1. Study cohort

In total, 120 participants were acquired in Freiburg, Munich, and Leipzig and included in this retrospective study. The study population comprised 30 patients with AD, 30 patients with FTD, 30 patients with LBD and 30 healthy controls (HC) with a minimum age of 60 years, respectively. Demographic and clinical data are given in Table 1. In order to avoid a confound between diagnostic category and scanning parameters, ten cases with AD, LBD, ten controls, and six cases with FTD were provided from Freiburg with comparable scanning parameters and supplemented with external data to fill each category. Participants from all diagnostic groups showed clinical and biomarker patterns (including 18F-FDG PET) consistent with their respective diagnosis according to established criteria. Specifically, HC were included

if their Montreal Cognitive Assessment (MoCA) score was  $\geq 26$  (Nasreddine et al., 2005) and their Beck's Depression Inventory-II (Beck et al., 1996) was  $\leq 13$ . This retrospective study was carried out in accordance with the latest update of the Declaration of Helsinki. HC MRI scans were approved by the local Medical Ethics Review Committee.

### 5.2. Image acquisition

Sagittal T1-weighted 3D magnetization prepared rapid gradient echo (MPRAGE) sequences (approximately  $1 \times 1 \times 1 \text{ mm}^3$  resolution) were acquired on different types of 1.5 and 3 Tesla Siemens scanners, each with a standard head coil (TR 2300–3000 ms, TE 2.86–4.0 ms, FA 8–9°, TI 900–1000 ms). The MPRAGE sequences were converted to NIfTI-2 format, and the filenames were pseudonymized before further processing.

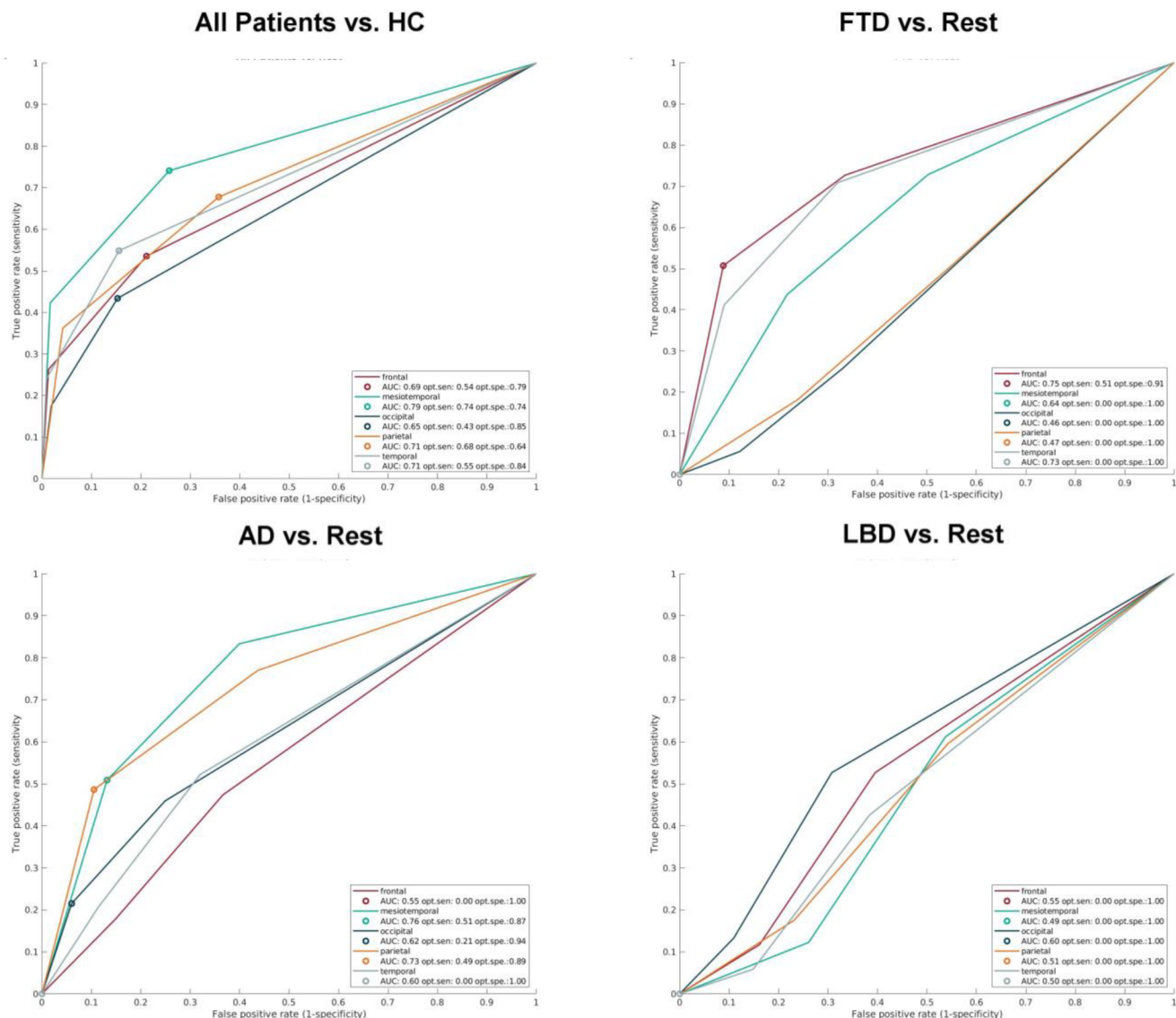


**Fig. 4.** ROC analyses of human rating based on established visual rating scales regarding frontal regions (red), medial (mesio) temporal regions (green), occipital regions (black), parietal regions (orange), and temporal regions (gray). Maximum sensitivity (opt. sen.) and maximum specificity (opt. spe.) is shown as small circle on the corresponding curve representing the intercept with a 45 degree line closest to the error-free point (0,1).

### 5.3. Visual rating

Visual rating was performed blinded for diagnoses. Atrophy in ten regions had to be rated on a three level scale (0 = normal; 1 = borderline atrophy; 2 = pathological atrophy). Medial temporal atrophy was adapted from the medial temporal atrophy score proposed by

Scheltens et al. (1992). The parietal atrophy rating followed the rating proposed by Koedam et al. (2011). Frontal and lateral temporal atrophy was rated following Davies et al. (2006). Occipital atrophy was evaluated concordant to the previously mentioned rating scales, since no standardized rating scale has been developed so far.

**Table 1**  
Sociodemographic characterization of the study cohorts.

	Healthy controls		Alzheimer's disease		Lewy-body dementia		Frontotemporal dementia	
	Mean	SD	Mean	SD	Mean	SD	Mean	SD
n (m/f)	13/17		14/16		14/16		11/19	
Age (years)	72.4	4.4	71.6	7.4	72.2	7.7	65.7	7.8
Education (years)	16.7	2.9	14.8	2.4	10.9	2.4	11.1	3.7
MMSE	29.0	1.5	23.2	3.2	22.1	3.2	22.8	3.4

Note: SD = standard deviation, MMSE = Mini Mental Status Examination.

For n = 6, no MMSE was available but cognitive functioning was evaluated with the Montreal Cognitive Assessment (MoCA). MoCA scores were converted into MMSE scores according to Trzepacz et al. (2015).

## 5.4. Image processing

### 5.4.1. Estimation of normalized local volumes

360 healthy controls (HC) were obtained from the Alzheimer's Disease Neuroimaging Initiative (ADNI) database (Weiner et al., 2010). As in patients the age of the healthy controls ranged from 55 to 90 years. All T1 weighted images were segmented into GM, WM and CSF and non-linear transformed to MNI space by using the segmentation algorithm of SPM12 (<http://www.fil.ion.ucl.ac.uk/spm/software/spm12>). The default setting was used for processing and the modulated warped tissues were selected as outputs. These normalized and modulated images were then smoothed with a Gaussian filter of 3x3x3 mm FWHM. The quantity of GM and CSF volume was adjusted linearly for effects of age, sex and total intracranial volume by using ordinary least squares estimation of regression parameters and the residual variance as estimate of uncertainty.

### 5.4.2. Calculation of atrophy scores

MRI data from all 120 study participants were processed analogous to the reference group with additional forward and inverse DARTEL transformation as outputs. The GM/CSF volumes were subtracted from the measured volume of 360 healthy controls. The atrophy scores  $\alpha_{GM}^{(v,s)}$  and  $\alpha_{CSF}^{(v,s)}$  for GM and CSF in MNI space were defined as:

$$\alpha^{(v,s)} = \frac{y^{(v,s)} - \bar{x}^s \hat{\beta}^v}{\hat{\sigma}^v}$$

where  $s$  indicate the subject and  $v$  voxel location.  $y$  is the measured local volume of GM or CSF,  $\bar{x}$  the predictors of age, sex and intracranial volume.  $\hat{\beta}$  is the estimated parameters of the linear model,  $\hat{\sigma}$  the estimated residual variance. These scores as map in MNI space were non-linear transformed back to native space. We used a threshold of  $-2$  for GM and  $2$  for CSF to display the atrophy scores, also called z-scores. The z-scores of CSF larger than  $2$  were displayed from red to yellow. The scores of GM less than  $-2$  were displayed from dark blue to light blue (see Fig. 1). The clusters of less than five voxels were removed from the map.

## 5.5. Evaluation and statistical analysis

Each of our 4 diagnoses was compared against the rest. To test for the diagnostic accuracy based on z-scores alone, we used the LPBA40 atlas (Shattuck et al., 2008) to define 10 regions of interest (ROI) (5 per hemisphere), covering frontal lobe, medial temporal structures (hippocampus, parahippocampal gyrus, entorhinal cortex), the rest of the temporal lobe (consecutively named "temporal region" for the sake of convenience) as well as covering parietal and occipital lobe structures. The corresponding ROIs were pooled across hemispheres and the mean z-score values, with the resulting volumes of voxels with abnormal z-scores ( $< -2$  for GM and  $> 2$  for CSF) within these ROIs were calculated. To define the diagnostic ability of this automated z-score based analysis, we showed the ROC curve with its resulting AUC as well as the sensitivity and specificity at optimized threshold settings derived from the intercept of the ROC curve with the line at 45 degrees closest to the error free point (0.1). According to an arbitrary guideline, we distinguished between non-informative (AUC = 0.5), less accurate ( $0.5 < AUC < 0.7$ ), moderately accurate ( $0.7 < AUC < 0.9$ ) and highly accurate ( $0.9 < AUC < 1$ ) (Swets, 1988).

## CRediT authorship contribution statement

**Karl Egger:** Conceptualization, Data curation, Methodology, Project administration, Writing - original draft. **Alexander Rau:** Data curation, Writing - review & editing. **Shan Yang:** Data curation, Formal analysis, Methodology, Software. **Stefan Klöppel:** Conceptualization, Data curation, Methodology, Project administration, Writing - review &

editing. **Ahmed Abdulkadir:** Conceptualization, Formal analysis, Methodology, Software. **Elias Kellner:** Formal analysis, Methodology, Project administration, Software. **Lars Frings:** Data curation. **Sabine Hellwig:** Conceptualization, Data curation. **Horst Urbach:** Methodology, Resources, Writing - review & editing. .

## Declaration of Competing Interest

The authors declare that they have no known competing financial interests or personal relationships that could have appeared to influence the work reported in this paper.

## Acknowledgement

**Funding:** This research did not receive any specific grant from funding agencies in the public, commercial, or not-for-profit sectors.

## References

- Ashburner, J., 2012. SPM: a history. *NeuroImage* 62, 791–800. <https://doi.org/10.1016/j.neuroimage.2011.10.025>.
- Beck, A.T., Steer, R.A., Ball, R., Ranieri, W., 1996. Comparison of beck depression inventories-IA and -II in psychiatric outpatients. *J. Pers. Assess.* 67, 588–597. [https://doi.org/10.1207/s15327752jpa6703\\_13](https://doi.org/10.1207/s15327752jpa6703_13).
- Cajanus, A., Hall, A., Koikkalainen, J., et al., 2018. Automatic MRI quantifying methods in behavioral-variant frontotemporal dementia diagnosis. *Dement. Geriatr. Cogn. Disord. Extra* 51–59. <https://doi.org/10.1159/000486849>.
- for the Alzheimer's Disease Neuroimaging Initiative, for the Alzheimer Precision Medicine Initiative (APMI)Cavedo, E., et al., 2017. Fully Automatic MRI-Based Hippocampus Volumetry Using FSL-FIRST: Intra-Scanner Test-Retest Stability, Inter-Field Strength Variability, and Performance as Enrichment Biomarker for Clinical Trials Using Prodromal Target Populations at Risk for Alzheimer's Disease. *J. Alzheimers Dis.* 60, 151–164. <https://doi.org/10.3233/JAD-161108>.
- Davies, R.R., Kipps, C.M., Mitchell, J., et al., 2006. Progression in frontotemporal dementia: identifying a benign behavioral variant by magnetic resonance imaging. *Arch. Neurol.* 63, 1627–1631. <https://doi.org/10.1001/archneur.63.11.1627>.
- Djukic, M., Wedekind, D., Franz, A., et al., 2015. Frequency of dementia syndromes with a potentially treatable cause in geriatric in-patients: analysis of a 1-year interval. *Eur. Arch. Psychiatry Clin. Neurosci.* 265, 429–438. <https://doi.org/10.1007/s00406-015-0583-3>.
- Fellhauer, I., Zöllner, F.G., Schröder, J., et al., 2015. Comparison of automated brain segmentation using a brain phantom and patients with early Alzheimer's dementia or mild cognitive impairment. *Psychiatry Res.* 233 (3), 299–305. <https://doi.org/10.1016/j.psychresns.2015.07.011>.
- Frenzel, S., Wittfeld, K., Habes, M., et al., 2020. (2020) A biomarker for Alzheimer's disease based on patterns of regional brain atrophy. *Front Psychiatry* 14 (10), 953. <https://doi.org/10.3389/fpsyg.2019.00953>.
- Frisoni, G.B., Boccardi, M., Barkhof, F., et al., 2017. Strategic roadmap for an early diagnosis of Alzheimer's disease based on biomarkers. *Lancet Neurol.* 16, 661–676. [https://doi.org/10.1016/S1474-4422\(17\)30159-X](https://doi.org/10.1016/S1474-4422(17)30159-X).
- Harper, L., Fumagalli, G.G., Barkhof, F., et al., 2016. MRI visual rating scales in the diagnosis of dementia: evaluation in 184 post-mortem confirmed cases. *Brain* 139, 1211–1225. <https://doi.org/10.1093/brain/aww005>.
- Hedderich, D.M., Dieckmeyer, M., Andrisan, T., et al., 2020. Normative brain volume reports may improve differential diagnosis of dementing neurodegenerative diseases in clinical practice. *Eur. Radiol.* <https://doi.org/10.1007/s00330-019-06602-0>.
- Huppertz, H.-J., Kröll-Seger, J., Klöppel, S., et al., 2010. Intra- and interscanner variability of automated voxel-based volumetry based on a 3D probabilistic atlas of human cerebral structures. *NeuroImage* 49, 2216–2224. <https://doi.org/10.1016/j.neuroimage.2009.10.066>.
- Huppertz, H.-J., Möller, L., Südmeyer, M., et al., 2016. Differentiation of neurodegenerative parkinsonian syndromes by volumetric magnetic resonance imaging analysis and support vector machine classification: classification of Parkinsonian Syndromes. *Mov. Disord.* 31, 1506–1517. <https://doi.org/10.1002/mds.26715>.
- Kazemi, Kamran, Noorizadeh, Negar, 2014. Quantitative comparison of SPM, FSL, and brainsuite for brain MR image segmentation. *J. Biomed. Phys. Eng.* 4, 13–26.
- Klöppel, S., Peter, J., Lüdt, A., et al., 2015. Applying automated MR-based diagnostic methods to the memory clinic: a prospective study. *J. Alzheimers Dis.* 47, 939–954. <https://doi.org/10.3233/JAD-150334>.
- Koedam, E.L.G.E., Lehmann, M., van der Flier, W.M., et al., 2011. Visual assessment of posterior atrophy development of a MRI rating scale. *Eur. Radiol.* 21, 2618–2625. <https://doi.org/10.1007/s00330-011-2205-4>.
- Meeter, L.H., Kaat, L.D., Rohrer, J.D., van Swieten, J.C., 2017. Imaging and fluid biomarkers in frontotemporal dementia. *Nat. Rev. Neurol.* 13, 406–419. <https://doi.org/10.1038/nrneurol.2017.75>.
- Möller, C., van der Flier, W.M., Versteeg, A., et al., 2014. Quantitative regional validation of the visual rating scale for posterior cortical atrophy. *Eur. Radiol.* 24, 397–404. <https://doi.org/10.1007/s00330-013-3025-5>.
- Muangpaisan, W., Petcharat, C., Srinonprasert, V., 2012. Prevalence of potentially reversible conditions in dementia and mild cognitive impairment in a geriatric clinic:

- reversible cognitive impairment/dementia. *Geriatr. Gerontol. Int.* 12, 59–64. <https://doi.org/10.1111/j.1447-0594.2011.00728.x>.
- Nasreddine, Z.S., Phillips, N.A., Bédirian, V., et al., 2005. The Montreal Cognitive Assessment, MoCA: a brief screening tool for mild cognitive impairment. *J. Am. Geriatr. Soc.* 53, 695–699. <https://doi.org/10.1111/j.1532-5415.2005.53221.x>.
- Nedelska, Z., Ferman, T.J., Boeve, B.F., et al., 2015. Pattern of brain atrophy rates in autopsy-confirmed dementia with Lewy bodies. *Neurobiol. Aging* 36, 452–461. <https://doi.org/10.1016/j.neurobiolaging.2014.07.005>.
- Persson, K., Barca, M.L., Cavallin, L., et al., 2017. Comparison of automated volumetry of the hippocampus using NeuroQuant® and visual assessment of the medial temporal lobe in Alzheimer's disease. *Acta Radiol.* <https://doi.org/10.1177/0284185117743778>.
- Saeed, U., Compagnone, J., Aviv, R.I., et al., 2017. Imaging biomarkers in Parkinson's disease and Parkinsonian syndromes: current and emerging concepts. *Transl. Neurodegener.* 6. <https://doi.org/10.1186/s40035-017-0076-6>.
- Scheltens, P., Leyns, D., Barkhof, F., et al., 1992. Atrophy of medial temporal lobes on MRI in "probable" Alzheimer's disease and normal ageing: diagnostic value and neuropsychological correlates. *J. Neurol. Neurosurg. Psychiatry* 55, 967–972. <https://doi.org/10.1136/jnnp.55.10.967>.
- Shattuck, D.W., Mirza, M., Adisetiyo, V., et al., 2008. Construction of a 3D probabilistic atlas of human cortical structures. *NeuroImage* 39, 1064–1080. <https://doi.org/10.1016/j.neuroimage.2007.09.031>.
- Swets, J.A., 1988. Measuring the accuracy of diagnostic systems. *Science* 240, 1285–1293.
- Trzepacz, P.T., Hochstetler, H., Wang, S., et al., 2015. Relationship between the Montreal Cognitive Assessment and Mini-mental State Examination for assessment of mild cognitive impairment in older adults. *BMC Geriatr.* 15, 107. <https://doi.org/10.1186/s12877-015-0103-3>.
- Weiner, M.W., Aisen, P.S., Jack, C.R., et al., 2010. The Alzheimer's disease neuroimaging initiative: progress report and future plans. *Alzheimers Dement J. Alzheimers Assoc.* 6, 202–211.e7. <https://doi.org/10.1016/j.jalz.2010.03.007>.
- Wippold, F.J., Brown, D.C., Broderick, D.F., et al., 2015. ACR appropriateness criteria dementia and movement disorders. *J. Am. Coll. Radiol.* 12, 19–28. <https://doi.org/10.1016/j.jacr.2014.09.025>.